Growth optimization of *Klebsiella pneumoniae* in magnetically assisted bioreactor

Maciej Konopacki[1,3*] , Adrian Augustyniak[1,2] , Bartłomiej Grygorcewicz[1,3] ,
Barbara Dołęgowska[3] , Marian Kordas[1] , Rafał Rakoczy[1]

[1]West Pomeranian University of Technology in Szczecin, Faculty of Chemical Technology
and Engineering, Department of Chemical and Process Engineering, al. Piastów 42,
71-065 Szczecin, Poland

[2]Technische Universität Berlin, Building Materials and Construction Chemistry, Gustav-Meyer Allee 25,
13355 Berlin, Germany

[3]Pomeranian Medical University in Szczecin, Chair of Microbiology, Immunology and Laboratory
Medicine, Department of Laboratory Medicine, al. Powstańców Wielkopolskich 72,
70-111 Szczecin, Poland

In recent years, infections are more often caused by pathogens with high multi-drug resistance, classified as the "ESKAPE" microorganisms. Therefore, investigation of these pathogens, e.g., *Klebsiella pneumoniae*, often requires biomass production for treatment testing such as antibiotics or bacteriophages. Moreover, *K. pneumoniae* can be successfully applied as a biocatalyst for other industrial applications, increasing the need for this bacteria biomass. In the current study, we proposed a novel magnetically assisted bioreactor for the cultivation of *K. pneumoniae* cells in the presence of an external alternating magnetic field (AMF). High efficiency of the production requires optimal bacteria growth conditions, e.g., temperature and field frequency. Therefore, we performed an optimization procedure using a central composite design for these two parameters in a wide range. As an objective function, we utilized a novel, previously described growth factor that considers both biomass and bacteria growth kinetics. Thus, based on the response surface, we could specify the optimal growth conditions. Moreover, we analysed the impact of the AMF on bacteria proliferation, which indicated positive field frequency windows, where the highest stimulatory effect of AMF on bacteria proliferation occurred. Obtained results proved that the magnetically assisted bioreactor could be successfully employed for *K. pneumoniae* cultivation.

Keywords: bacteria cultivation; growth kinetics; optimization process; magnetically assisted bioreactor

1. INTRODUCTION

Klebsiella pneumoniae is well known as a pathogen causing nosocomial infections. World Health Organization considers particularly strains resistant to antibiotics as one of the main threats to global healthcare (Kollef et al., 2014; Tacconelli et al., 2018). Investigating the biology and pathogenesis of this microorganism often requires the production of its biomass, which could be later used for the studies of host-pathogen

---

www.czasopisma.pan.pl   PAN   www.journals.pan.pl

Maciej Konopacki et al.   Chem. Process Eng., 2022, 43 (3), 289–304

interactions, diagnostic test manufacturing, or as an inoculum for the production of lytic bacteriophages that are often proposed as a solution for various bacterial contamination in medicine, natural environment and industry (Grygorcewicz et al., 2020; Grygorcewicz et al., 2017; Sybesma et al., 2016). Recently, also other biotechnological uses for *K. pneumoniae* biomass were proposed. One of the most extensively studied applications of this bacterium is the possibility to use it as a bio-catalyst for industrial biotechnology in the production of industrially essential acids and alcohols from glycerol (Chen et al., 2015; Kumar and Park, 2018; Mitrea and Vodnar, 2019; Qin et al., 2006; Rehman et al., 2021; Sabra et al., 2016; Sun et al., 2021). Nevertheless, it should be highlighted that *K. pneumoniae* is a dangerous pathogen and when it is possible, a non-pathogenic bacteria strain should be used instead (e.g. *C. butyricum* in diol production).

On the other hand, new methods allowing high-yield biomass production are still sought. The stimulation of the living organisms for intensifying the biotechnological process can be induced by various factors (Domingues et al., 2000; Fijałkowski et al., 2016; Konopacka et al., 2019). Apart from the common optimization steps such as adjustments of temperature, pH, substrates, and aeration, novel possibilities are being explored (Askitosari et al., 2019; Derakhshandeh and Tezcan Un, 2019; Leili et al., 2020; Medina-Cabrera et al., 2020). One promising approach is applying external (magnetic, electric, or ultrasound) force fields. So far, the electromagnetic field has been used for biomass or enzyme production, intensification of biochemical processes, and enzymatic reactions. However, this application is still under examination, both theoretically and experimentally (Al-Qodah et al., 2017; Konopacki et al., 2021; Lechowska et al., 2019; Rakoczy et al., 2017a; Rakoczy et al., 2017b; Wang et al., 2017; Zhang et al., 2017). One of the currently investigated studies is the idea of alternating magnetic field application (AMF, e.g., rotating magnetic field, RMF) for bioprocess intensification. While many observations in this subject have been made on model microorganisms, i.e., *E. coli* and *S. aureus* in magnetically assisted bioreactors (Konopacki and Rakoczy, 2019; Struk et al., 2017), there is still not much data on the optimization of *K. pneumoniae* in such conditions. Our previous study proposed a novel mathematical description to optimize bacteria growth (Konopacki et al., 2020). Previously, we have analysed only the temperature impact on *K. pneumonia* proliferation. In the current stage of the project, we have utilized a magnetically assisted bioreactor. Thus the impact of the additional parameter connected with the AMF, along with temperature, should be tested. Therefore, this study aimed at finding optimal thermal and field conditions for the production of *K. pneumoniae* biomass in a magnetically assisted bioreactor, which was not reported before.

2. MATERIALS AND METHODS

2.1. Bacterial strain cultivation parameters

In the present study, a reference strain of *Klebsiella pneumoniae* (ATCC® BAA-1706™) was employed (biosafety BSL-2 – pathogenic strain that can cause mild disease to humans). Before use, bacteria were kept frozen (–21 °C) in Trypticase Soy Broth medium (TSB) with 10% (v/v) glycerol. Fresh bacterial cultures were used, and the material was not passaged to new media more than five times. The fresh inoculum was used for every experiment.

Cultures were incubated at 37 °C for 24 h at Trypticase Soy Agar (TSA) medium. In the next step, a colony was transferred to 30 mL of fresh TSB medium and incubated overnight (14-16 h) at 37 °C. Afterward, 300 mL of TSB (that was kept at the test temperature) was inoculated in (1:100) and dispensed to Falcon tubes (10 mL of inoculum to each tube). Starting from the inoculum (at $t = 0$), 8 samples (100 μL each) were taken to measure optical density (OD, at $\lambda_{OD} = 600$ nm) on BioTek Synergy H1 (Winooski, VT, USA) spectrophotometer. The experiments were continued for 10 hours in aerobic conditions to achieve the stationary phase. At each time point (every hour), one tube was taken from each bioreactor and used to prepare eight samples (100 μL each) subjected to OD measurements. The cultivation was led in

various temperatures and electromagnetic field frequencies given by the experiment's design and control temperature conditions (without the electromagnetic field marked as $f = 0$ Hz). Moreover, to confirm gained tendencies, all experiments were triplicated. Within each experiment, all harvested samples were studied in eight repetitions.

Furthermore, cell metabolic activity (respiration) was measured in resazurin assay, as described elsewhere (Augustyniak et al., 2020). Resazurin assay was prepared by loading 10 µL of resazurin (1 mg/mL in PBS) to each well. Afterward, the samples were incubated at $34\,°C$ for 20 min, and the fluorescence ($\lambda_{ex} = 520$ nm and $\lambda_{em} = 590$ nm) read on spectrophotometer BioTek Synergy H1 (BioTek, Winooski, VT, USA).

2.2. Experimental setup

The schematic of the experimental setup is presented in Fig. 1. The experimental setup consists of two identical bioreactors. The single system has a tank (1) where the RMF generator (2) is placed in the form of a 3-phase stator. Inside the generator, a water bath made of polycarbonate (3) is situated. The samples with bacterial cultures (4) are placed on a sample rack inside the container around its axis at the same distance from the wall. The RMF is generated by the 3-phase AC supplied and controlled through the phase inverter (5) connected with the PC (6). The RMF is formed due to the superposition of electromagnetic fields generated by every phase coil situated around the same axis. The RMF generator during work produces heat due to the electric resistance of coils powered by AC. For that reason, the generator is submerged in silicone oil (an electric isolator) which allows to transport the heat outside the tank with the oil circulation pump (7). The heat produced by the generator can be used again to maintain the cultivation tank temperature. Excessive heat can be removed from the system through the plate heat exchanger (8). The amount of heat within the water stream transported back to the tank is controlled by the control valve (9) equipped with the temperature sensor.
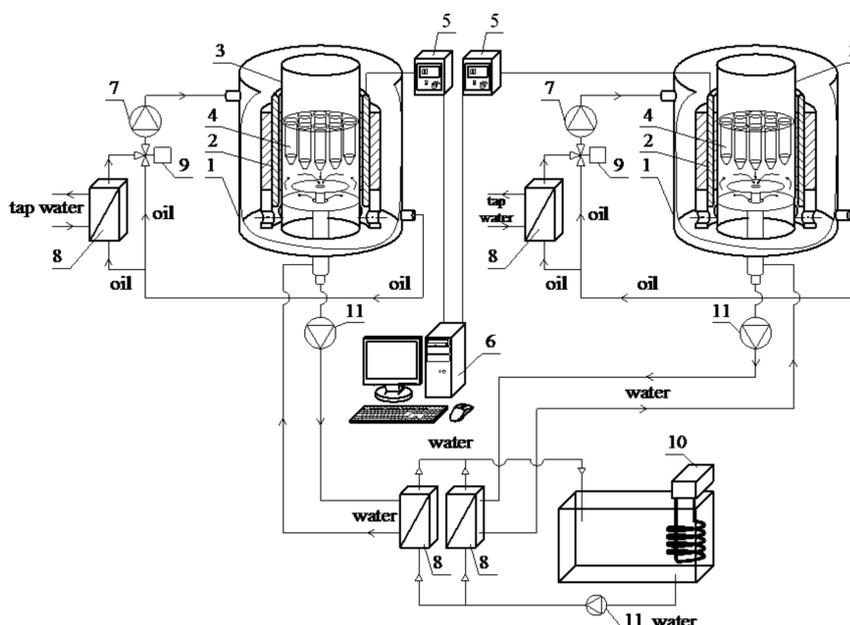

Fig. 1. Schematic of the experimental setup: 1 – bioreactor tank, 2 – RMF generator, 3 – polycarbonate container, 4 – 3-phase inverter, 5 – PC, 6 – sample, 7 – control valve, 8 – plate heat exchanger, 9 – oil circulation pump, 10 – thermostat, 11 – water circulation pump

However, in this study, we decided to mount an additional temperature control system. We applied a precise thermostat (10) filled with distilled water to maintain the demanded temperature level. Water from the

www.czasopisma.pan.pl PAN www.journals.pan.pl

Maciej Konopacki et al. Chem. Process Eng., 2022, 43 (3), 289–304

thermostat was transported by the circulation pump (11) to a set of two heat exchangers, where the water bath from each cultivation container was heated to the needed temperature (the same in both bioreactors). This system allowed to control the temperature within the bioreactors very precisely (changes below 0.1 °C). Moreover, in case of some fluctuation of temperature, it affected both bioreactors simultaneously; thus, the temperature difference between bioreactors can be neglected.

The RMF magnetic flux density (B) measurements were performed using the FW Bell 5180 digital gaussmeter for the whole range of utilized field frequency, proportional to frequency f of power current (5–50 Hz). It should be noticed that the power frequency is the controlled parameter (using the AC inverter) and the magnetic flux density varies with the changes of frequency. The typical magnetic field distribution in the generator area is presented in Fig. 2.
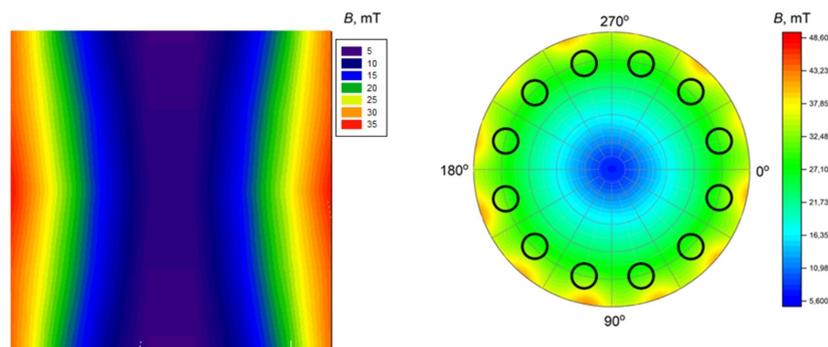

Fig. 2. Typical distribution of magnetic flux density in the RMF generator: a) vertical cross-section, b) horizontal cross-section at the position of the samples (f = 30 Hz)

The RMF distribution presented in Fig. 2 was found to be symmetrical around the generator axis. The highest magnetic flux density values were measured near the generator's wall and decreased toward the center. Samples with the cell suspension were placed around the generator axis in the uniform field zone (black circles, respecting to Fig. 2), creating the same field conditions in each sample.

2.3. Design of experiments

The optimization of the *K. pneumoniae* growth conditions was planned with the design of the experiment (DoE) technique utilizing the central composite design. In this study, we decided to test bacteria growth under RMF exposure at various temperatures. Therefore, two parameters were selected for optimization, i.e., the temperature (x_1) and the frequency (x_2). The input matrix containing the standardized values of each parameter is presented in Table 1.

Table 1. Central composite design input matrix

Experiment	1	2	3	4	5	6	7	8	9
x_1	1	1	−1	−1	0	0	0	a	−a
x_2	1	−1	1	−1	0	a	−a	0	0
y	y_1	y_2	y_3	y_4	y_5	y_6	y_7	y_8	y_9

where: x_1, x_2 – input parameters, y – the objective function.
Values of each parameter:
x_1: "−a" = 32 °C, "−1" = 33.5 °C, "0" = 37 °C, "1" = 40.5 °C, "a" = 42 °C,
x_2: "−a" = 5 Hz, "−1" = 11.6 Hz, "0" = 27.5 Hz, "1" = 43.4 Hz, "a" = 50 Hz.

Furthermore, the experimental points given by the composition plan were extended by the additional five points, for each tested temperature without the RMF presence ($f = 0$ Hz). The objective function should be chosen according to the purpose of the experiment, i.e. microorganism growth kinetics, biomass or product concentration. The objective function values measured in the experiments can be described as a function of two input parameters, commonly by the quadratic model, defined by the following equation:

$$y(x_1, x_2) = p_0 + p_1 x_1 + p_2 x_2 + p_3 x_1 x_2 + p_4 x_1^2 + p_5 x_2^2 \qquad (1)$$

where: p_0–p_5 – equation parameters.

Estimation of Eq. (1) parameters allows us to find the objective function extremum, thus finding the optimal values of the input parameters. In other words, we can find optimal values of the input parameters (such as process conditions) for which we can obtain maximized or minimized value of specified objective function. In the current study, we aimed to optimize *K. pneumoniae* growth based not only on amount of biomass, but on the growth kinetics. Therefore, we decided to use as an objective function a newly proposed parameter, we called growth factor, that evaluates the whole bacterial growth curve. The growth parameter takes into account the whole growth process – both kinetics and final biomass concentration. The detailed information about growth factor was described in our previous manuscript (Konopacki et al., 2020). In the present study, growth factor calculations are shown in *Evaluation of bacteria growth* section.

3. RESULTS AND DISCUSSION

3.1. Evaluation of bacteria growth

The bacteria growth was monitored through the optical density (OD) measurements. The typical changes of the OD during the process are presented in Fig. 3.
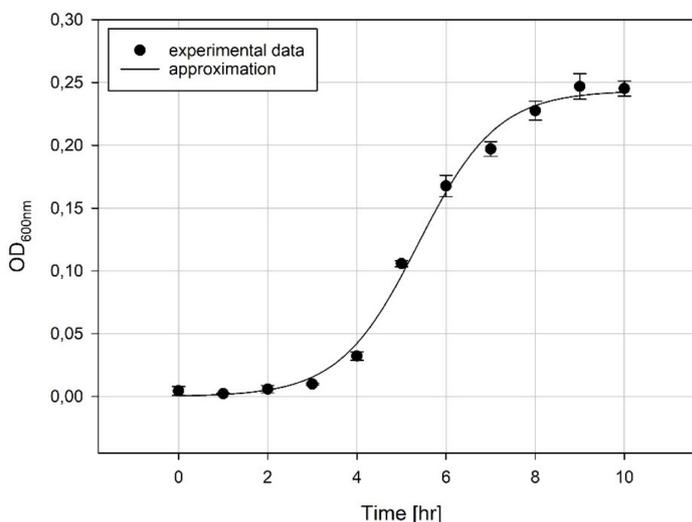

Fig. 3. A typical bacteria growth curve ($f = 27.5$ Hz, $T = 37\,°$C)

The growth curve presented in Fig. 3 has a characteristic sigmoidal shape so that it can be precisely approximated by the following logistic equation:

$$\mathrm{OD}(t) = \frac{a}{1 + \exp(b - ct)} \qquad (2)$$

where: a [–], b [–], c [hr^{-1}] – Eq. (2) coefficients, t – time [hr].

www.czasopisma.pan.pl　PAN　www.journals.pan.pl

Maciej Konopacki et al.   Chem. Process Eng., 2022, 43 (3), 289–304

All growth curves obtained in the experiments were approximated with Eq. (2) using Statistica 13 (Statsoft, Poland). Precision of adjustment was described by the coefficient of determination, R^2. Therefore, the estimated values of a, b, c and R^2 coefficients are presented in Table 2.

Table 2. Estimated values of Eq. (2) coefficients for each growth curve

T [°C]	f [Hz]	a [–]	b [–]	c [hr^{-1}]	R^2
32	0	0.2419	7.6118	1.1533	0.9983
32	27.5	0.2416	7.1500	1.0754	0.9984
33.5	0	0.2418	6.6310	1.1847	0.9972
33.5	11.6	0.2680	5.0749	1.0685	0.9865
33.5	43.4	0.2652	5.1236	1.0108	0.9928
37	0	0.2192	5.2081	1.1774	0.9879
37	5	0.2137	6.2425	1.2274	0.9888
37	27.5	0.2436	5.1027	1.1655	0.9943
37	50	0.2179	4.5026	1.1451	0.9862
40.5	0	0.1929	4.6595	1.0967	0.9899
40.5	11.6	0.1987	5.1531	1.2812	0.9900
40.5	43.4	0.2178	6.3902	1.2346	0.9917
42	0	0.1708	5.8127	1.5672	0.9849
42	27.5	0.1876	4.5764	1.1368	0.9874

The bacterial growth was described using a few parameters such as the maximum specific growth rate, maximum concentration of biomass, or the duration of the lag-phase (Zwietering et al., 1990). Knowing the values of Eq. (2) coefficients (Table 2), it was possible to estimate the value of each growth parameter (Konopacki et al., 2020). The specific growth rate was calculated as follows:

$$\mu_{\max} = \frac{ac}{4} \ \left[\text{hr}^{-1}\right] \tag{3}$$

The following equation defined the lag-phase duration:

$$\lambda = \frac{b - 2}{c} \ [\text{hr}] \tag{4}$$

The maximum biomass concentration (treated as the asymptote A of the sigmoidal curve) was defined as:

$$A = a \ [-] \tag{5}$$

Each of those above mentioned parameters can be used as the objective function for the optimization process. Nevertheless, choosing only a single parameter that does not fully describe the bacteria growth phenomenon may lead to severe errors in estimating growth conditions. On the other hand, multi-parametric optimization can be complicated and demand an advanced mathematical approach. Therefore, in one of our

previous manuscripts, we proposed a single parameter that assumes all those three parameters we called the growth factor (Konopacki et al., 2020):

$$\varphi = n_A \left(1 - \frac{b}{ct}\right) \; [-], \quad n_A = \frac{A}{A_{\max}} \tag{6}$$

where: n_A – maximum growth ratio, $A_{\max}$ – maximum value of the asymptote estimated for the whole data set.

As a result, the values of the maximum specific growth rate, $\mu_{\max}$, duration of the lag-phase, λ, maximum biomass concentration, A, and the growth factor, φ, are presented in Fig. 4 as the contour plot versus temperature and frequency.

Fig. 4. Bacteria growth in tested conditions (from Eq. (3–6): a) the maximum biomass concentration, b) lag-phase duration, c) maximum specific growth rate, d) growth factor

The results presented in Fig. 4 indicate that every parameter covered a different area with an optimal range of values. Current results have confirmed our previous finding that the maximum biomass concentration given by the asymptote (Fig. 4a) is achieved in the temperature between 33–35 °C (Konopacki et al., 2020). This result confirms that the reference temperature (37 °C) commonly used for culturing *K. pneumoniae* is not optimal. The RMF with frequency in the 20–40 Hz range had the most potent effect on bacterial growth.

www.czasopisma.pan.pl PAN www.journals.pan.pl

Maciej Konopacki et al. Chem. Process Eng., 2022, 43 (3), 289–304

Moreover, higher temperatures (38–42 °C) assisted with RMF produced a more considerable stimulatory effect, particularly in the middle of the frequency region, creating a specific positive "window". Such frequency "windows" were reported previously (Ahmed et al., 2013; Binhi and Savin, 2002; Carta and Desogus, 2012), although we have observed this effect along with the temperature changes in the current work. The duration of lag-phase (Fig. 4b) decreased with the temperature reaching a relatively low value at 34 °C. Moreover, the RFM significantly influenced λ values in the range 15–40 Hz at 34–37 °C and up to 25 Hz at 40–42 °C.

The maximum specific growth rate (Fig. 4c) was primarily affected by the temperature. The increasing RMF intensity caused a relatively slight inhibition of the specific growth rate. The highest μ_{max} values can be observed at 33–35 °C and frequency up to 20 Hz. Literature data suggest that the highest biochemical activity of these bacteria is between 30–35 °C (Grimont and Grimont, 2015), which supports our finding.

Those three described parameters covered different regions with optimal values, suggesting the specificity of observed effects. This knowledge could be used depending on the purpose accompanying the bacterial cultures. Furthermore, it means that other values of the parameters could be used to achieve higher maximum biomass concentration (Fig. 4a), shorter lag-phase duration (Fig. 4b), or maximum specific growth rate (Fig. 4c). Nevertheless, we have based our optimization on the growth factor considering all the above parameters, allowing us to choose the proper growth conditions. The results presented in Fig. 4d suggest that the optimal growth can be obtained for the temperature at the range between 34–36 °C and RMF exposure of frequency in the range 25–35 Hz.

3.2. Optimization of K. pneumoniae cultivation conditions

To estimate accurate optimal temperature and frequency, we utilized the growth factor as the objective function for Eq. (1). Moreover, in the current study, we modified Eq. (1) by substituting the additional reciprocal terms $\frac{p_6}{T}$, $\frac{p_7}{T^2}$ to provide sufficient surface curvature and lower the adjustment error. Finally, the growth factor as the function of temperature and frequency was defined as follows:

$$\varphi(T, f) = p_0 + p_1 T + p_2 f + p_3 T f + p_4 T^2 + p_5 f^2 + \frac{p_6}{T} + \frac{p_7}{T^2} \tag{7}$$

The non-linear estimation of Eq. (7) parameters was performed with Statistica 13 software (Statsoft, Poland). The quasi-Newton method was employed with the quadratic loss function (mean square error, MSE, where MSE $= \dfrac{\sum_{i=1}^{n}(y_i - \hat{y}_i)^2}{n}$). The quasi-Newton method uses the estimated values of first and second-order derivatives to analyse how fast and in which direction the function slope is changing. This information is then utilized to minimize the loss function. The estimated parameters of Eq. (6) allowed to create a surface plot (called a response surface) $\phi(T, f)$ with marked data points that are presented in Fig. 5. Parameters $p_0 - p_7$ of Eq. (7) are presented in Table 3.

Table 3. Estimated parameters of the Eq. (6)

p_0	p_1	p_2	p_3	p_4	p_5	p_6	p_7	R^2
–2.60E+03	4.54E+01	1.25E–02	–2.96E–01	–6.12E–05	–2.50E–04	6.62E+04	–6.30E+05	0.90

The obtained parameters presented in Table 3 allowed us to optimize the function given by Eq. (6). In this study, the optimization was conducted with Matlab 2020b software (Mathworks, USA). Our optimization aim was to maximize the growth factor value. However, most of the mathematical procedures available in
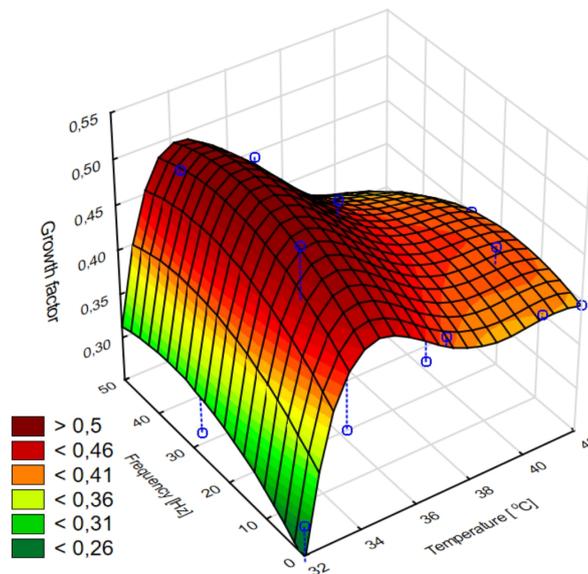
Fig. 5. Surface plot of the adjusted growth factor $\phi(T, f)$ function to the experimental data

the software give the only possibility to minimize the non-linear multivariable function. For that reason, the *fmincon* – built-in Matlab algorithm finding the function minimum was applied for the $-\phi(T, f)$ function (this is equal to maximize $\phi(T, f)$) with boundaries set to the analysed region ($T = 32$–$42\,°C$, $f = 0 - 50$ Hz). This procedure allowed us to obtain the optimal values of both temperature and frequency for the maximized growth factor. The optimized parameters are presented in Table 4.

Table 4. Optimized values of temperature and frequency

Parameter	Optimal value
Temperature [°C]	34.38
Frequency [Hz]	31.51

Based on the calculated optimal conditions, we performed an additional experiment to verify the correctness of the model. The results are presented in Fig. 6 and Table 5.
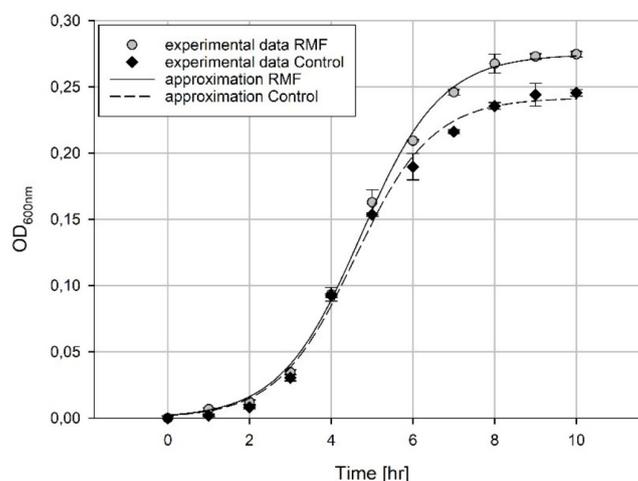

Fig. 6. *K. pneumoniae* growth in optimized conditions with and without the impact of RMF

www.czasopisma.pan.pl PAN www.journals.pan.pl

Maciej Konopacki et al. Chem. Process Eng., 2022, 43 (3), 289–304

Table 5. Growth factor for optimized conditions

	RMF	Control	RMF predicted	Error
Growth factor	0.500	0.451	0.515	3%

Results presented in Fig. 6 (for the optimized growth conditions) show the difference in growth after 5 hours of exposure. The EMF action possibly allowed for the avoidance of limitations resulting in higher biomass concentration in the stationary phase. This effect could be created by changes in reactive oxygen species generation (ROS) during exposure. We reported recently that RMF exposure could lead to subtle changes in the ROS level in cells (Jabłońska et al., 2022). ROS can affect metabolic performance, e.g. regulating some physiological processes, or impact utilized metabolic routes. However, this mechanism was not proven enough, so more studies are required.

3.3. Impact of RMF on K. pneumoniae growth

To study the impact of RMF exposure on *K. pneumoniae* growth in various temperatures, we compared the growth factor calculated for the whole data set obtained for experiments with various RMF frequencies and the control process (without the exposure). The results are presented in Table 6 as growth stimulation index given by the following equation:

$$G_s = \frac{\varphi_{\mathrm{RMF}} - \varphi_{\mathrm{Control}}}{\varphi_{\mathrm{Control}}} \cdot 100\% \tag{8}$$

where: ϕ_{RMF} – growth factor for the process with RMF exposure, ϕ_{Control} – growth factor for the process without the RMF exposure in the same temperature.

Table 6. Growth stimulation index for tested cases

T [°C]	f [Hz]	G_s [%]
32	27.5	−2.72
33.5	11.6	31.41
33.5	43.4	32.75
37	5	−10.92
37	27.5	11.33
37	50	4.19
40.5	11.6	−11.35
40.5	43.4	8.08
42	27.5	1.48
34.4	31.5	9.80

Data presented in Table 6 showed the highest stimulatory effect of RMF at 33.5 °C for the tested frequencies. On the contrary, at 37 °C, the RMF effect strongly depended on the applied RMF frequency, where the most significant positive effect was observed for 27.5 Hz, which was close to the calculated optimal frequency.

The highest and lowest temperature from the analysed range (32 and 42 °C) yielded no significant changes compared to the control process without the external electromagnetic field. For the middle-temperature range (33.5–40.5 °C) various effect of RMF exposure was observed; thus temperature had the major impact on bacteria growth. Moreover, in general, we can see that frequencies at the middle range gave the best stimulatory effect, whereas low frequency showed the inhibitory effect. These findings also confirm the assumption of possible positive and negative frequency windows (Ahmed et al., 2013). It should be highlighted that the G_s index shows only the difference in growth between the control and exposed bacteria, which is not identical with the maximum possible growth found for the optimal conditions.

The calculated optimal growth conditions were validated by testing the bacteria metabolic activity for tested ranges of temperature and frequency. Cell metabolic activity was measured in resazurin assay, which allowed us to estimate the ratio between samples treated with rotating magnetic field (RMF) and controls with the following equation:

$$E_{\mathrm{RMF}} = \frac{M_{\mathrm{RMF}} - M_{\mathrm{Control}}}{M_{\mathrm{Control}}} \cdot 100\% \tag{9}$$

where: M – metabolic activity, E – effectiveness of rotating magnetic field stimulation [%].

A single time point (4 h), common for all used conditions where bacteria were in the exponential growth phase, was selected for further analysis. A contour plot in Fig. 7 presents these findings.
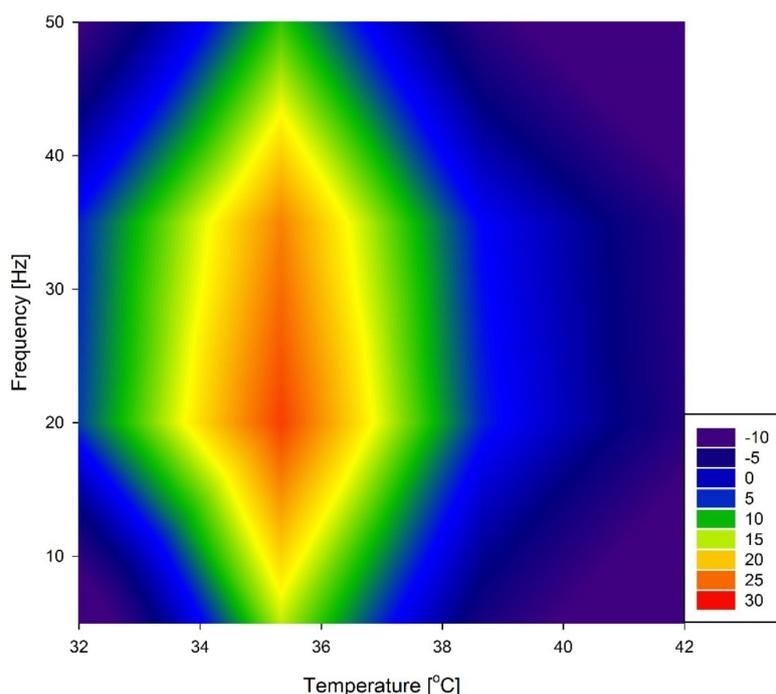

Fig. 7. Values of the effectiveness factor, E_{RMF} (Eq. (9)) of the cell metabolic activity stimulation in various temperatures

The results presented in Fig. 7 indicated that in the temperatures of 32–38 °C under RMF exposure bacteria respiration was higher than in the controls. This stimulatory effect was highest between 34 and 36.5 °C. Moreover, we also observed inhibition of the cell proliferation for low (up to 20 Hz) and high (40–50 Hz) field frequency for the higher temperature. Thus, the values found during these studies (T = 34.4 °C, f = 31.5 Hz) showed one of the significant improvements of the metabolic activity stimulation relating to the control process. However, it should be noticed that the data presented in Fig. 7 were given for a single point (4 h) and cannot describe the whole growth process like the proposed growth factor. Thus, the electromagnetic field mechanisms that impact the bacteria cell proliferation are still not well described.

www.czasopisma.pan.pl   PAN   www.journals.pan.pl

Maciej Konopacki et al.   Chem. Process Eng., 2022, 43 (3), 289–304

Various groups speculated about the action mechanism for electromagnetic fields. One of the most common assumptions is that the electromagnetic field may generate oxidative stress in cells. It was found, e.g., in mitochondria of eukaryotic cells (Santini et al., 2018). Our results from the resazurin assay indicate that this could be the case in our studies. Blue resazurin pigment is reduced by NAD(P)H-dependent reductases (Hall et al., 2016). Furthermore, Lemire et al. (2017) have shown that oxidative stress may stimulate overproduction of NADPH which would explain the higher fluorescence in samples exposed to RMF. Another hypothesis suggested that the electromagnetic field is creating eddy currents which, in principle, may increase the availability of nutrients to growing cells or increase the aeration of the culture medium (Aubert et al., 2012; Hammond, 1962; Hristov, 2010).

Another leading theory implies the modification of the cell membrane transport by facilitating the penetration of the relatively large ions (e.g., divalent cations of metals), magneto- and electroporation effect, and the micro-mixing phenomena induced by the magnetic field (Konopacki and Rakoczy, 2019). Similar findings of AMF impact on cell transport mechanism were recently suggested for the *Saccharomyces cerevisiae* yeast model. De Andrade et al. (2021) discussed the possible biophysical effect of electromagnetic fields that may influence the transport of H^+ ions. If the same effect would accompany EMF action in *K. pneumoniae*, it might influence the proton-motive force crucial for energy production (ATP) in bacteria (Roger et al., 2018). However, in bacteria, this hypothesis should be verified by some additional research involving gene expression and metabolic pathway studies. At this point, it is possible to obtain the positive effect of the electromagnetic field exposure on the bacteria growth but for the particular conditions which can be used in further processing, e.g., production of the bacteriophages.

The optimization of the *K. pneumoniae* cultivation process was the first stage of our current project. Then, the optimized biomass production will be further studied in bacteriophage production. Previously we discovered that the application of AMF (B = 34 mT, f = 50 Hz) improved the induction of lambdoid prophages (Struk et al., 2017). In further studies, we will verify whether the observed stimulation of bacteria can be applied in the more efficient production of lytic phages. For that reason, we plan to set up a very promising two-stage magnetically assisted process of bacteriophage production, where at the first stage, AMF will stimulate the host-cell proliferation and alter their metabolic activity, and at the second stage, AMF will facilitate the phage adsorption and cell infection.

4. CONCLUSIONS

We have successfully conducted the optimization of *K. pneumoniae* growth in the planned experimental conditions. The central composite design of experiments limited the total number of conducted experiments. We found that the measured parameters: maximum specific growth rate, duration of lag-phase, and maximum concentration of biomass showed different optimal regions; thus, the optimization could be complicated. These difficulties were mitigated through using the previously proposed growth factor as an objective function. We confirmed that the *K. pneumoniae* growth was optimal near 34 °C. An external electromagnetic field did not significantly change the optimal temperature. However, we found that the field with about 30 Hz frequency could stimulate bacterial growth in the optimal temperature up to 10%, which confirmed the possibility of increasing the effectiveness of the process using certain AMF. In this study, we found optimal temperature lower than reference, commonly used 37 °C. Additionally, this will result in decreased energy consumption, thus reducing the bioprocess's operational cost.

SYMBOLS

a	logistic function coefficient,
A	growth curve asymptote,
$A_{\max}$	maximum value of growth asymptote,
b	logistic function coefficient,
c	logistic function coefficient, hr^{-1}
E	effectiveness of rotating magnetic field stimulation, %
f	frequency, Hz
G_s	growth stimulation index, %
M	metabolic activity
n_A	maximum growth ratio,
p	equation parameter,
T	temperature, °C
x	input parameter,
y	objective function,

Greek symbols

$\mu_{\max}$	maximal specific growth rate, hr^{-1}
λ	lag-phase duration, hr
λ_{em}	fluorescence emission wavelength, nm
λ_{ex}	fluorescence excitation wavelength, nm
λ_{OD}	optical density wavelength, nm
φ	growth factor,

Subscripts

1, 2	number of parameter
Control	for process without electromagnetic field exposure,
RMF	for process with electromagnetic field exposure

REFERENCES

Ahmed I., Istivan T., Cosic I., Pirogova E., 2013. Evaluation of the effects of Extremely Low Frequency (ELF) Pulsed Electromagnetic Fields (PEMF) on survival of the bacterium *Staphylococcus aureus*. *EPJ Nonlinear Biomed. Phys.*, 1, 5. DOI: 10.1140/epjnbp12.

Al-Qodah Z., Al-Shannag M., Al-Busoul M., Penchev I., Orfali W., 2017. Immobilized enzymes bioreactors utilizing a magnetic field: A review. *Biochem. Eng. J.*, 121, 94–106. DOI: 10.1016/j.bej.2017.02.003.

Askitosari T.D., Boto S.T., Blank L.M., Rosenbaum M.A., 2019. Boosting heterologous phenazine production in *Pseudomonas putida* KT2440 through the exploration of the natural sequence space. *Front. Microbiol.*, 10, 1990. DOI: 10.3389/fmicb.2019.01990.

Aubert G., Jacquinot J.-F., Sakellariou D., 2012. Eddy current effects in plain and hollow cylinders spinning inside homogeneous magnetic fields: Application to magnetic resonance. *J. Chem. Phys.*, 137, 154201. DOI: 10.1063/1.4756948.

Augustyniak A., Sikora P., Jabłońska J., Cendrowski K., John E., Stephan D., Mijowska E., 2020. The effects of calcium–silicate–hydrate (C–S–H) seeds on reference microorganisms. *Appl. Nanosci.*, 10, 4855–4867. DOI: 10.1007/s13204-020-01347-5.

Binhi V.N., Savin A.V., 2002. Molecular gyroscopes and biological effects of weak extremely low-frequency magnetic fields. *Phys. Rev. E*, 65, 051912. DOI: 10.1103/PhysRevE.65.051912.

www.czasopisma.pan.pl   PAN   www.journals.pan.pl

Maciej Konopacki et al.   Chem. Process Eng., 2022, 43 (3), 289–304

Carta R., Desogus F., 2012. Possible non-thermal microwave effects on the growth rate of *Pseudomonas Aeruginosa* and *Staphylococcus Aureus*. *Int. Rev. Chem. Eng.*, 4(4), 392–398.

Chen Z., Sun H., Huang J., Wu Y., Liu D., 2015. Metabolic engineering of *Klebsiella pneumoniae* for the production of 2-butanone from glucose. *PLoS ONE*, 10, e0140508. DOI: 10.1371/journal.pone.0140508.

de Andrade C.M., Cogo A.J.D., Perez V.H., dos Santos N.F., Okorokova-Façanha A.L., Justo O.R., Façanha A.R., 2021. Increases of bioethanol productivity by *S. cerevisiae* in unconventional bioreactor under ELF-magnetic field: New advances in the biophysical mechanism elucidation on yeasts. *Renewable Energy*, 169, 836–842. DOI: 10.1016/j.renene.2021.01.074.

Derakhshandeh M., Tezcan Un U., 2019. Optimization of microalgae *Scenedesmus SP*. growth rate using a central composite design statistical approach. *Biomass Bioenergy*, 122, 211–220. DOI: 10.1016/j.biombioe.2019.01.022.

Domingues L., Vicente A.A., Lima N., Teixeira J.A., 2000. Applications of yeast flocculation in biotechnological processes. *Biotechnol. Bioprocess Eng.*, 5, 288–305. DOI: 10.1007/BF02942185.

Fijałkowski K., Żywicka A., Drozd R., Junka A.F., Peitler D., Kordas M., Konopacki M., Szymczyk P., El Fray M., Rakoczy R., 2016. Increased yield and selected properties of bacterial cellulose exposed to different modes of a rotating magnetic field. *Eng. Life Sci.*, 16, 483–493. DOI: 10.1002/elsc.201500151.

Grimont P.A.D., Grimont F., 2015. *Klebsiella*, In: Whitman W.B. et al. (Eds.), *Bergey's manual of systematics of archaea and bacteria.* Willey, New York, 1–26. DOI: 10.1002/9781118960608.gbm01150.

Grygorcewicz B., Chajęcka-Wierzchowska W., Augustyniak A., Wasak A., Stachurska X., Nawrotek P., Dołęgowska B., 2020. In-milk inactivation of *Escherichia coli* O157:H7 by the environmental lytic bacteriophage ECPS-6. *J. Food Saf.*, 40, e12747. DOI: 10.1111/jfs.12747.

Grygorcewicz B., Grudziński M., Wasak A., Augustyniak A., Pietruszka A., Nawrotek P., 2017. Bacteriophage-mediated reduction of *Salmonella* Enteritidis in swine slurry. *Appl. Soil Ecol.*, 119, 179–182. DOI: 10.1016/j.apsoil.2017.06.020.

Hall M.D., Simeonov A., Davis M.I., 2016. Avoiding fluorescence assay interference-The case for diaphorase. *ASSAY Drug Dev. Technol.*, 14, 3, 175–179. DOI: 10.1089/adt.2016.707.

Hammond P., 1962. The calculation of the magnetic field of rotating machines. Part 3: Eddy currents induced in a solid slab by a circular current loop. *Proc. IEE – Part C: Monographs*, 109, 508–515. DOI: 10.1049/pi-c.1962.0066.

Hristov J., 2010. Magnetic field assisted fluidization – a unified approach.Part 8. Mass transfer: Magnetically assisted bioprocesses. *Rev. Chem. Eng.*, 26, 55–128. DOI: 10.1515/REVCE.2010.006.

Jabłońska J., Augustyniak A., Kordas M., Dubrowska K., Sołoducha D., Borowski T., Konopacki M., Grygorcewicz B., Roszak M., Dołęgowska B., Piz M., Filipek E., Wróbel R.J., Leniec G., Rakoczy R., 2022. Evaluation of ferrofluid-coated rotating magnetic field-assisted bioreactor for biomass production. *Chem. Eng. J.*, 431, 133913. DOI: 10.1016/J.CEJ.2021.133913.

Kollef M.H., Chastre J., Fagon J.-Y., François B., Niederman M.S., Rello J., Torres A., Vincent J.-L., Wunderink R.G., Go K.W., Rehm C., 2014. Global prospective epidemiologic and surveillance study of ventilator-associated pneumonia due to *Pseudomonas aeruginosa**. *Crit. Care Med.*, 42, 2178–2187. DOI: 10.1097/CCM.0000000000000510.

Konopacka A., Rakoczy R., Konopacki M., 2019. The effect of rotating magnetic field on bioethanol production by yeast strain modified by ferrimagnetic nanoparticles. *J. Magn. Magn. Mater.*, 473, 176–183. DOI: 10.1016/j.jmmm.2018.10.053.

Konopacki M., Augustyniak A., Grygorcewicz B., Dołęgowska, B., Kordas, M., Rakoczy R. 2020. Single mathematical parameter for evaluation of the microorganisms' growth as the objective function in the optimization by the doe techniques. *Microorganisms*, 8, 1706. DOI: 10.3390/microorganisms8111706.

Konopacki M., Rakoczy R., 2019. The analysis of rotating magnetic field as a trigger of Gram-positive and Gram-negative bacteria growth. *Biochem. Eng. J.*, 141, 259–267. DOI: 10.1016/j.bej.2018.10.026.

Konopacki, M., Jędrzejczak-Silicka, M., Szymańska, K., Mijowska, E., Rakoczy, R., 2021. Effect of rotating magnetic field on ferromagnetic structures used in hyperthermia. *J. Magn. Magn. Mater.*, 518, 167418. DOI: 10.1016/j.jmmm.2020.167418.

Kumar V., Park S., 2018. Potential and limitations of *Klebsiella pneumoniae* as a microbial cell factory utilizing glycerol as the carbon source. *Biotechnol. Adv.,* 36, 150–167. DOI: 10.1016/j.biotechadv.2017.10.004.

Lechowska J., Kordas M., Konopacki M., Fijałkowski K., Drozd R., Rakoczy R., 2019. Hydrodynamic studies in magnetically assisted external-loop airlift reactor. *Chem. Eng. J.*, 362, 298–309. DOI: 10.1016/j.cej.2019.01.037.

Leili M., Shirmohammadi K.N., Godini K., Azarian G., Moussavi R., Peykhoshian A., 2020. Application of central composite design (CCD) for optimization of cephalexin antibiotic removal using electro-oxidation process. *J. Mol. Liq.*, 313, 113556. DOI: 10.1016/j.molliq.2020.113556.

Lemire J., Alhasawi A., Appanna V.P., Tharmalingam S., Appanna V.D., 2017. Metabolic defence against oxidative stress: the road less travelled so far. *J. Appl. Microbiol.*, 123, 798–809. DOI: 10.1111/jam.13509.

Medina-Cabrera E.V., Rühmann B., Schmid J., Sieber V., 2020. Optimization of growth and EPS production in two *Porphyridium* strains. *Bioresour. Technol. Rep.*, 11, 100486. DOI: 10.1016/j.biteb.2020.100486.

Mitrea L., Vodnar, D.C., 2019. *Klebsiella pneumoniae* – a useful pathogenic strain for biotechnological purposes: Diols biosynthesis under controlled and uncontrolled pH levels. *Pathogens*, 8, 293. DOI: 10.3390/pathogens8040293.

Qin J., Xiao Z., Ma C., Xie N., Liu P., Xu P., 2006. Production of 2,3-butanediol by *Klebsiella Pneumoniae* using glucose and ammonium phosphate. *Chin. J. Chem. Eng.*, 14, 132–136. DOI: 10.1016/S1004-9541(06)60050-5.

Rakoczy R., Lechowska J., Kordas M., Konopacki M., Fijałkowski K., Drozd R., 2017a. Effects of a rotating magnetic field on gas-liquid mass transfer coefficient. *Chem. Eng. J.*, 327, 608–617. DOI: 10.1016/j.cej.2017.06.132.

Rakoczy R., Przybył A., Kordas M., Konopacki M., Drozd R., Fijałkowski K., 2017b. The study of influence of a rotating magnetic field on mixing efficiency. *Chem. Eng. Process. Process Intensif.*, 112, 1–8. DOI: 10.1016/j.cep.2016.12.001.

Rehman S., Khairul I.M., Khalid K.N., Kyoungjin A.A., Chaiprapat S., Leu, S.Y., 2021. Whole sugar 2,3-butanediol fermentation for oil palm empty fruit bunches biorefinery by a newly isolated Klebsiella pneumoniae PM2. *Bioresour. Technol.*, 333, 125206. DOI: 10.1016/j.biortech.2021.125206.

Roger M., Brown F., Gabrielli W., Sargent F., 2018. Efficient hydrogen-dependent carbon dioxide reduction by *Escherichia coli*. *Curr. Biol.*, 28, 140–145. DOI: 10.1016/j.cub.2017.11.050.

Sabra W., Groeger C., Zeng A.P., 2016. Microbial cell factories for diol production, In: Ye Q., Bao J., Zhong J.J. (Eds.), *Bioreactor engineering research and industrial applications I. Advances in biochemical engineering/biotechnology*. Springer, Berlin, Heidelberg. 155, 165–197. DOI: 10.1007/10_2015_330.

Santini S.J., Cordone V., Falone S., Mijit M., Tatone C., Amicarelli F., Di Emidio G., 2018. Role of mitochondria in the oxidative stress induced by electromagnetic fields: Focus on reproductive systems. *Oxid. Med. Cell. Longevity*, 2018, 5076271. DOI: 10.1155/2018/5076271.

Struk M., Grygorcewicz B., Nawrotek P., Augustyniak A., Konopacki M., Kordas M., Rakoczy R., 2017. Enhancing effect of 50 Hz rotating magnetic field on induction of Shiga toxin-converting lambdoid prophages. *Microb. Pathogen.*, 109, 4–7. DOI: 10.1016/j.micpath.2017.05.018.

Sun S., Shu L., Lu X., Wang Q., Tišma M., Zhu C., Shi J., Baganz F., Lye G.J., Hao, J., 2021. 1,2–Propanediol production from glycerol via an endogenous pathway of *Klebsiella pneumoniae*. *Appl. Microbiol. Biotechnol.*, 105, 23, 9003–9016. DOI: 10.1007/s00253-021-11652-w.

Sybesma W., Zbinden R., Chanishvili N., Kutateladze M., Chkhotua A., Ujmajuridze A., Mehnert U., Kessler T.M., 2016. Bacteriophages as potential treatment for urinary tract infections. *Front. Microbiol.*, 7, 465, 1–9. DOI: 10.3389/fmicb.2016.00465.

Tacconelli E., Carrara E., Savoldi A., Harbarth S., Mendelson M., Monnet D.L., Pulcini C., Kahlmeter G., Kluytmans J., Carmeli Y., Ouellette M., Outterson K., Patel J., Cavaleri M., Cox E.M, Houchens C.R, Grayson M.L., Hansen P., Singh N., Theuretzbacher U., Magrini N., The WHO Pathogens Priority List Working Group, 2018. Discovery, research, and development of new antibiotics: the WHO priority list of antibiotic-resistant bacteria and tuberculosis. *Lancet Infect. Dis.*, 18, 318-327. DOI: 10.1016/S1473-3099(17)30753-3.

www.czasopisma.pan.pl   PAN   www.journals.pan.pl

Maciej Konopacki et al.   Chem. Process Eng., 2022, 43 (3), 289–304

Wang Z., Liu X., Ni S.Q., Zhang J., Zhang X., Ahmad H.A., Gao B., 2017. Weak magnetic field: A powerful strategy to enhance partial nitrification. *Water Res.*, 120, 190–198. DOI: 10.1016/j.watres.2017.04.058.

Zhang X., Yarema K., Xu A., 2017. Impact of static magnetic field (SMF) on microorganisms, plants and animals. In: *Biological effects of static magnetic fields*. Springer Singapore, 133–172. DOI: 10.1007/978-981-10-3579-1.

Zwietering M.H., Jongenburger I., Rombouts F.M., van't Riet K., 1990. Modeling of the bacterial growth curve. *Appl. Environ. Microbiol.*, 56, 1875–1881. DOI: 10.1128/aem.56.6.1875-1881.1990.